Influence of sliver nanoparticles from thrush Candida albicans supernatant against Escherichia coli, Klebsiella pneumoniae, and Proteus mirabilis

Nour Radhi Saud[1*], Mouna Akeel Hamed Al-Oebady[1]

[1] *Department of biology, College of science, Al-Muthanna University, Samawah 66001, Iraq*

[*] *Corresponding Author: nourradee@mu.edu.iq*

Received 5 June. 2025, Accepted 16 July. 2025, published 30 Dec. 2025.

DOI: 10.52113/2/12.02.2025/112-126

Abstract: This study presents an eco-friendly method for synthesizing silver nanoparticles (AgNPs) using the supernatant of *Candida albicans* as a reducing agent. AgNPs were formed via redox reactions and characterized by X-ray diffraction (XRD), field emission scanning electron microscopy (FESEM), and atomic force microscopy (AFM). XRD analysis confirmed a face-centered cubic structure. The antibacterial activity of AgNPs was evaluated against three Gram-negative bacteria—*Escherichia coli*, *Klebsiella pneumoniae*, and *Proteus mirabilis*—using the agar well diffusion method. Their efficacy was compared to four antibiotics: Imipenem (IPM), Amoxicillin/clavulanic acid (AMC), Meropenem (MRP), and Piperacillin/tazobactam (PIT). While antibiotics were effective against *K. pneumoniae* and *P. mirabilis*, *E. coli* showed resistance to PIT and AMC. In contrast, AgNPs exhibited concentration-dependent inhibition, with maximum zones of 16.00 ± 0.58 mm (*K. pneumoniae*), 27.00 ± 0.57 mm (*P. mirabilis*), and 22.33 ± 0.33 mm (*E. coli*). These findings suggest AgNPs as promising antibacterial agents.

Keywords: antimicrobial, *Candida. albicans,* green synthesis, nanoparticles, silver.

1. Introduction

Currently, the rising incidence of infectious illnesses caused by multidrug-resistant (MDR) bacteria is a significant global public health challenge [1]. The MDR bacteria response to antimicrobial agents fundamentally illustrates adaptation and evolutionary behavior [2]. Chromosomal mutations or horizontal gene transfer lead to the evolution of antibiotic resistance in bacteria, a naturally occurring phenomenon observable in the absence of human intervention [3]. Non-traditional antibacterial agents are omit it significant interest in addressing antibiotic resistance

for various pathogenic germs, as the rising prevalence of MDR bacteria necessitates alternative therapies [4] .

Nanotechnology has demonstrated potential as an alternative to traditional antibiotics in treating MRD bacterial infections by offering innovative strategies for medicine administration, antibacterial treatment, and the development of new nanomaterials [5] [6]. Heavy metals with a density over 5 g/cm³ are commonly utilized to synthesis antibacterial nanoparticles (NPs) [7]. Their partially filled d orbitals as transition metals augment redox activity, enabling nanoparticle manufacturing via a "bottom-up" method that incorporates metal salts and reducing agents such as sodium borohydride [8].

While necessary in minimal quantities, certain metals become hazardous at elevated concentrations. Nanoparticles progressively discharge metal ions that infiltrate cells and disrupt biological functioning [9]. Their antibacterial capabilities arise from the generation of reactive oxygen species (ROS) and their interaction with R-SH groups in amino acids (e.g., cysteine), which disrupts enzyme activity and protein stability, particularly in non-essential metals such as Ag^{+}, leading to cellular harm [10].

Silver nanoparticles (AgNPs) can be synthesized using chemical, physical, or biological methods, typically categorized into top-down and bottom-up approaches. The bottom-up approach, which primarily utilizes chemical and biological methods, synthesizes AgNPs by assembling molecular components via nucleation and growth [11]. Chemical methods facilitate rapid production of AgNPs; however, their use in medical applications may be constrained by the presence of chemical additives. Biological methods present a viable alternative to address these challenges [12].

In green chemistry, biological synthesis has surfaced as a practical and cost-effective alternative, this approach offers advantages as it does not necessitate organic solvents and can be conducted at ambient temperature and pressure [13]. The dual role of biological systems as stabilizing and reducing agents is particularly advantageous for the formation of AgNPs [12]. This process can be supported by various species, including fungi, bacteria, yeast, algae, and plants [14]. This study utilized a reducing agent derived from Candida albicans to synthesis silver nanoparticles, which were then tested for their antimicrobial efficacy against three Gram-negative bacteria.

2. Methodology (Experimental Procedure)

2.1. Materials and Chemicals

All chemicals, including silver nitrate (99.9%) and ethanol (99.0%), were obtained from Reagent World \ California USA and utilized without additional purification. MacConkey Agar, blood agar, nutrient broth agar, Mueller Hinton agar, Mueller Hinton broth ,eosin methylene blue agar, Brain Heart Infusion Broth, CHROM agar, Sabouraud dextrose agar , Sabouraud dextrose broth and corn meal agar were obtained from Himedia. Imipenem (IMP), Ampicillin-clavulanate (AMC), Piperacillin/Tazobactam (PIT), and Meropenem (MRP) were acquired from Himedia\ India .

2.2 Collection and Identification of sample

Between September and December 2024 , a total of 30 yeast isolates were obtained following collection and isolation from children suffering from thrush at Al-Samawa Children's Teaching Hospital in Al-Muthanna governorate , Iraq. 27 isolates has been identified as *C. albicans* by application of CHROM agar, biochemical assays, microscopic analysis, and Gram staining. *C. albicans* strain was subsequently chosen for the biosynthesis of silver nanoparticles [15]. At the same time, 20 samples were collected from women's urine to investigate the presence of *K. pneumoniae, E. coli, and P. mirabilis*. Isolates were collected from patients within the same hospital. The isolates were subsequently identified through Gramm staining, microscopic examination, biochemical tests, and the use of culture media [16].

2.3 Preparation of *Candida albicans* Supernatant

The fresh colonies of *C. albicans* omit it from thrush were activated by stabbing in Sabouraud dextrose broth and subsequently cultured on 10 plates of Sabouraud Dextrose agar (SDA) using a cotton swab via the spreading method to achieve full growth. The plates were incubated for 48 hours at 37°C. Supernatant was harvested by soaking each of the 10 plates with 10 ml of deionized water, ensuring that colonies were collected without scraping the SDA. 100 ml of *C. albicans* supernatant was collected in a clean sterilized bottle and incubated for 72 hours at 37°C with a shaking speed of 150 rpm in a shaker incubator. Subsequently, the supernatant was centrifuged for 15 minutes at 4000 rpm to eliminate the yeast cell. A 0.22 µm Millipore syringe filter was employed for additional filtration, and the resulting solution was stored at 4°C until required, sines all of isolates gathering from same place and same pathogenic case all of

isolates were used successfully with synthesis of AgNPs excluded of yeast that non albicans species . This preparation technique was modified from an earlier published methodology with specific adjustments [17].

2.4. Synthesis of the Ag-NPs

The subsequent process employed for the fabrication of the alternative green synthesis of Ag-NPs is outlined below. Initially, 70 mL of the C. albicans extract was judiciously added dropwise to 930 mL of AgNO3 (1 mM) while being heated to 60°C and stirred for 1 hour in a dark environment. The reduction of Ag+1 ions was aged for 10 days to ensure complete nucleation and stabilization of Ag-NPs. The brownish colloidal solution was ultimately separated via centrifugation (12000 rpm, 15 minutes) to isolate the black precipitate, utilizing ethanol and deionized water [18]. The Ag-NPs precipitate was carefully purified until the supernatant was clear by washing it with deionized water. Subsequently, the Ag-NPs precipitate was dried for 3 hours at 60 °C in the oven [19].

2.5. Characterization AgNPs

Using a Hitachi S-4800 diffractometer and CuKα radiation (0.15040 nm), the crystalline phase of AgNPs was described by XRD. The XRD pattern was recorded between 20 and 70° [20]. The electronic microscope (FESEM-MIRA3 TESCAN)and AFM were utilized to observe the morphological characteristics of AgNPs [21].

2.6. Antibacterial Activity

The Mueller-Hinton Agar well diffusion method was employed to measure the diameter of the inhibitory zone and assess the *in vitro* antibacterial efficacy of the resultant AgNPs. The current work utilized Gram-negative bacteria, specifically *K. pneumoniae, P. mirabilis,* and *E. coli*, to assess antibacterial effects [22]. The procedure entailed inoculating freshly subculture bacterial strains into Muller-Hinton broth, incubating for 24 hours at 37°C, and thereafter correcting the turbidity to 0.5 McFarland standards. An agar well diffusion method was utilized to evaluate the antibacterial characteristics of the nanoparticles. Seventy microliters of the colloidal nanoparticle product were introduced into wells formed in the Muller-Hinton agar use a sterile borer with a 6 mm diameter. After a 24-hour incubation at 37°C, the diameter of the growth-inhibiting zones on the plates were measured and compared effect of antibiotic [23].

2.7. Antibiotics Susceptibility Test

Antibiotic sensitivity testing was conducted using Kirby-Bauer disc diffusion [24] .

Antibiotics include: (IPM), (PIT), and (AMC) were among those taken into consideration (CLSI, 2023)

2.8. Minimum Inhibitory Concentration (MIC) and Minimum Bactericidal Concentration (MBC) Evaluation

The antibacterial efficacy of silver nanoparticles was evaluated using the conventional broth dilution method, which is based on CLSI M07-A8 criteria. From a solution of silver nanoparticles with a starting concentration of 1 mg/ml, a series of decimal (tenfold) dilutions was made. To get a bacterial suspension with half the turbidity of 0.5 McFarland standard, the concentration was adjusted to around 5×10^7 CFU/ml. A soup called Brain Heart Infusion (BHI) was utilised as the container. The modified bacterial suspension was added to each dilution and left to incubate at 37 °C for 24 hours. There was also a control tube for growth that contained infected broth but no nanoparticles. A bacterial growth-free zone was identified as the minimal inhibitory concentration (MIC) when silver nanoparticles were used at the lowest concentration. The MIC endpoint was confirmed by evaluating visual turbidity before and after incubation.

Following the MIC assessment of the silver nanoparticles, 50 µl aliquots from all tubes exhibiting no visible bacterial growth were inoculated onto BHI agar plates and incubated for 24 hours at 37 °C. The MBC endpoint is defined as the lowest concentration of an antimicrobial agent that eradicates 99.9% of the bacterial population.

2.9. Statistical analyses

Statistical analyses were performed using SPSS software version 24. The means were compared using the *t*-test at a significance level of 0.001, and descriptive statistics were applied to calculate the standard deviation at the same significance threshold. Differences in the mean inhibition zone diameters were assessed using Duncan's Multiple Range Test (DMRT).

3. Results and Discussion

3.1 Identification of *Candida albicans*

As in figure.1 *C. albicans* isolate were identified by SDA agar , Chrom agar , Corn meal agar to investigate present of Chlamydospore under microscope, and investigate produce germ tube[25].

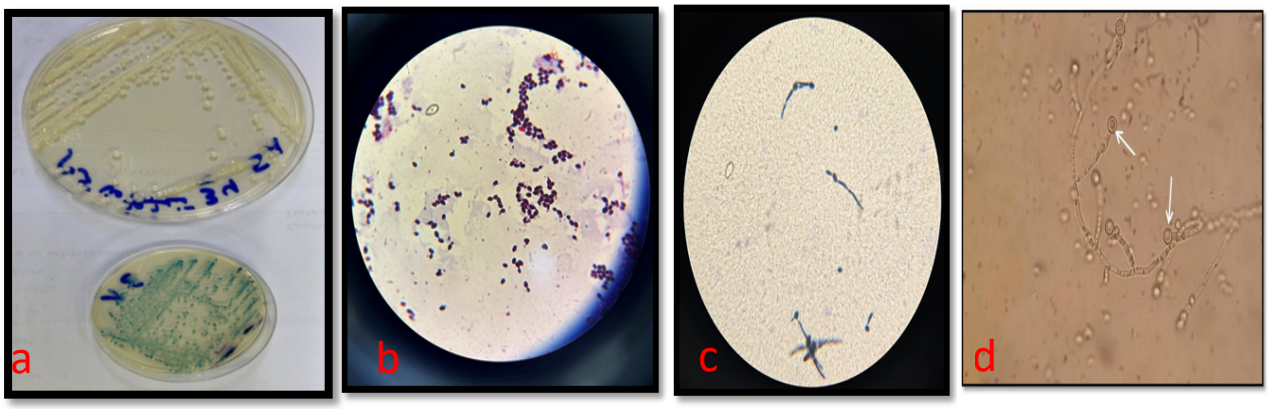

Fig.1: a) C. albicans on SAD agar and on Chrom agar b) C. albicans under microscope b) Germ tube under microscope d) Chlamydospore under microscope.

3.2 Identification of bacteria

Escherichia coli, Klebsiella pneumoniae, and *Proteus mirabilis* were identified by traditional media and biochemical test as in Fig.2 and Fig.3.

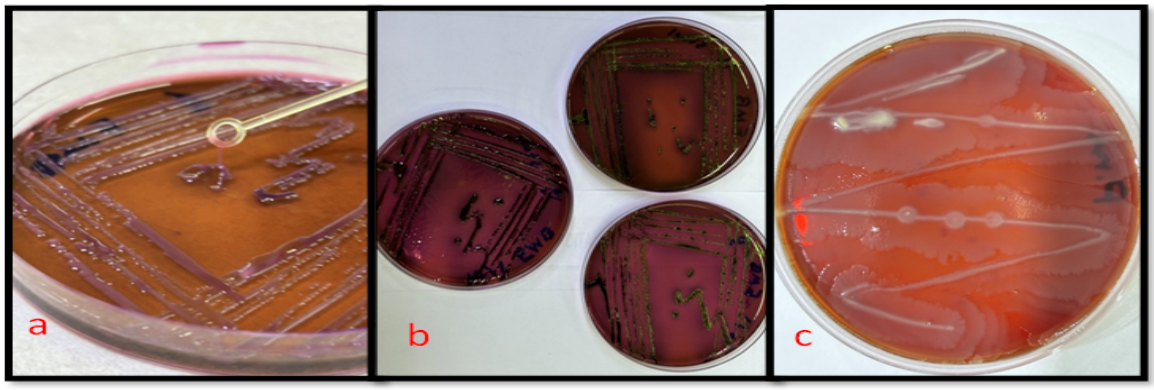

Fig.2: **a)** *K. pneumoniae,* on MacConkey agar showed mucoid colony [26] **b)** *E.coli* on EMB agar showed metallic shine [27] **c**) *P. mirabilis* on blood agar showed swarming movement [28]

Fig.3: Biochemical test result of a) *K. pneumoniae* b) *E.coli* and c) *P. mirabilis*

3.3 Color of AgNPs solution

The biosynthesis of silver nanoparticles using the cell-free supernatant of *Candida albicans* was visually monitored through a noticeable color change over time. Initially, the silver nitrate ($AgNO_3$) solution appeared colorless (Figure 4-a). Upon the addition of the *C. albicans* supernatant, the reaction mixture gradually shifted to a pale yellow hue (Figure 4-b), indicating the onset of silver ion reduction. As the reaction progressed, a distinct reddish-brown coloration developed (Figure 4-c), confirming the formation of colloidal silver nanoparticles [29].

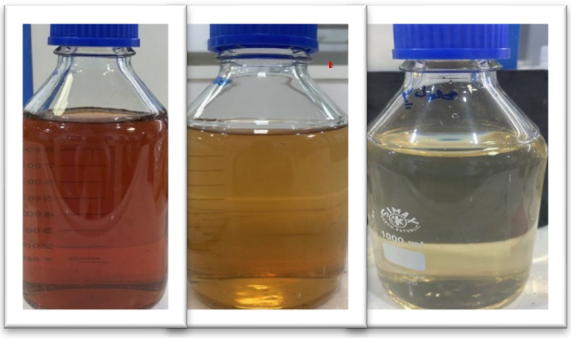

Fig.4. Color change observed during the time-dependent biosynthesis of silver nanoparticles: (a) initial silver nitrate solution, (b) intermediate stage after reaction with the biological extract, and (c) final colloidal AgNPs.

3.4 X-ray diffraction

Figure 5 demonstrates that XRD analysis was employed to evaluate the crystalline quality and lattice characteristics of the green-synthesized AgNPs. The XRD diffractogram displays diffraction peaks of the synthesized AgNPs within the 2θ range of 20°–70°, specifically at 27.73°, 32.15°, 38.01°, 46.16°, and 57.35°. These peaks correspond to the (h, k, l) Miller indices of (110), (111), (121), (200), and (311), respectively. The observed values align with JCPDS file number 84-0713 and may be associated with the face-centered cubic structure of AgNPs [30]. Several unidentified peaks (*) may be associated with the crystallization of biomolecules on the surface of AgNPs [31]. The average crystalline size of the AgNPs was calculated to be 29.27 nm on the (111) plane utilizing Scherrer's formula, expressed as $D = 0.9\lambda/\beta \cos\theta$ [32]. D represents the average crystallographic size (Å), denotes the source of X-ray radiation (λ = 1.54 Å), indicates the finite line full width at half maximum (FWHM), and θ signifies Bragg's angle in this formula [33].

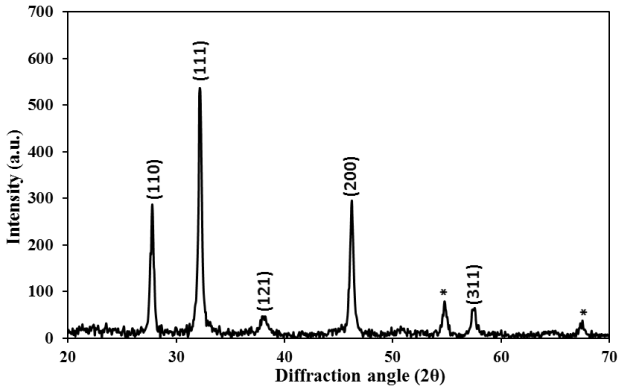

Fig.5. XRD pattern of synthesized AgNPs with candida albcans supernantant.

3.5. Field Emission Scanning Electron Microscope

Figure 6 illustrates the examination of surface morphology and particle distribution of

AgNPs using FESEM. The semi-spherical shape observed in the FESEM image is associated with AgNPs that have aggregated, forming particles that adhere together with varying sizes between (50-100) nm.

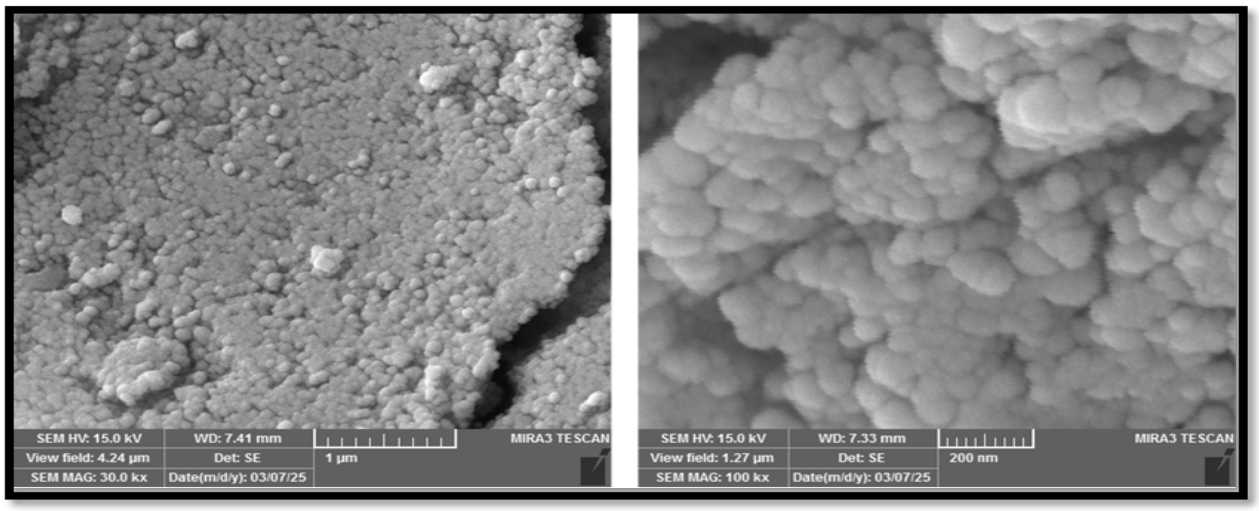

Fig.6. FESEM images of AgNPs

3.6 Atomic force microscopy

The surface morphology of AgNPs was analyzed using AFM. Figure 7 displays a three-dimensional image of AgNPs captured in tapping mode. The AFM image reveals a highly uniform distribution of spherical particles. Statistical roughness analysis (CSPM) indicates a surface skewness of 0.16890, a surface kurtosis of 3.239, and a root mean square roughness of 4.252 nm. The AFM findings indicate that the surface of the AgNPs is characterized by spikes, with valleys being more pronounced than peaks, and irregularities predominantly located in the middle regions[34]. Figure 3 demonstrates that AgNPs fall within the nanoscale range, as indicated by the histogram of their average particle size.

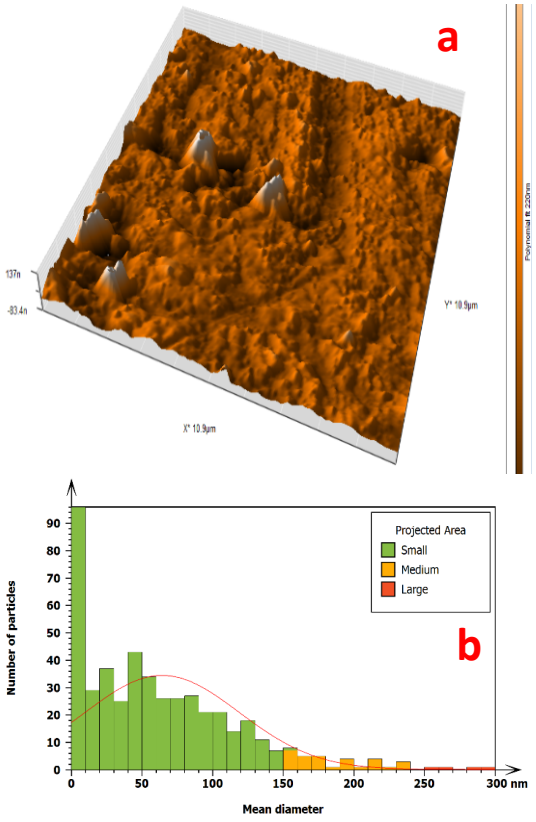

Fig.7. AFM image of AgNPs and with particle analysis histogram.

3.7. Antibacterial Activity results

The preliminary investigation of the antibacterial efficacy of AgNPs was performed utilizing the agar well diffusion technique. The AgNPs and four competing antibiotics (IPM, AMC, MRP, and PIT) exhibited notable zones of inhibition against the three examined pathogens (*K. pneumoniae, E. coli, and P. mirabilis*). Table 1 and Figures 8 ,9 illustrate the inhibition zones of antibiotics and AgNPs against each examined bacterium. In Figure 4, IMP, AMC, MRP, and PIT, utilized as a positive control, exhibited considerable antibacterial activity with varying inhibition zones (refer to Table 1) against *K. pneumoniae and P. mirabilis*; however, PIT and AMC shown antibacterial resistance to *E. coli*. As illustrated in Figure 5, these three bacteria treated with AgNPs exhibited concentration-dependent inhibitory zones [35]. Table 2 illustrates that the maximum inhibition zones were 15mm and 22mm at 100 ppm and 1000 ppm for *K. pneumoniae and E. coli*, respectively, while P. mirabilis exhibited a maximum inhibition zone of 26mm at both values of 1000 ppm. The minimum inhibitory concentration (MIC) of silver nanoparticles (AgNPs) against gram-negative bacteria was 100 ppm which has been demonstration by well 96 microplate assay [36] .

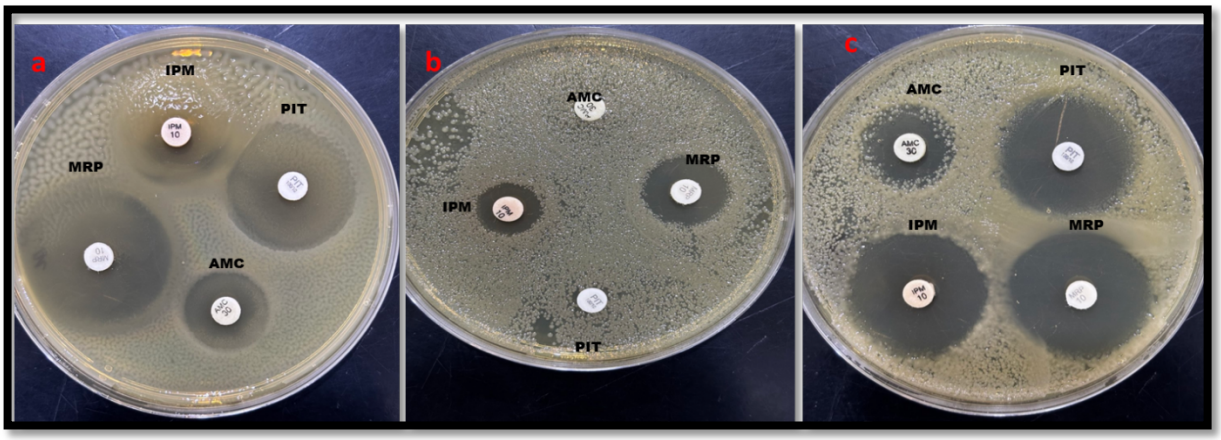

Fig .8. Antibiotics Susceptibility against a) *P. mirabilis* b) *E.coli* and c) *K. pneumonia.*

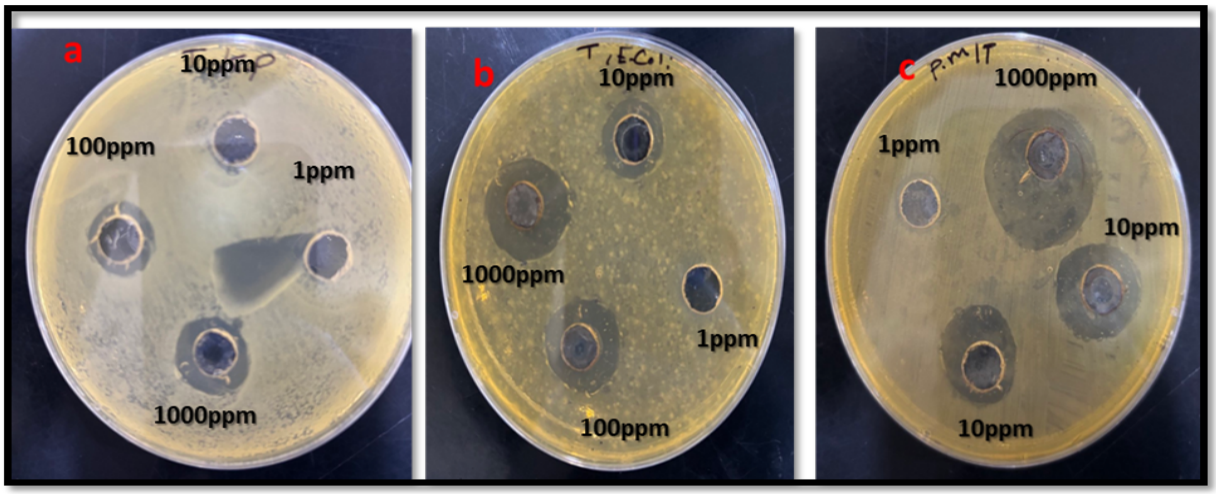

Fig.9. Inhibition zone of AgNPs against (a) *K. pneumoniae* (b) *E . coli* (c) *P .mirabilis*

Table 1. Inhibition zone diameter of four antibiotics against *K. pneumoniae, E.coli,* and *P. mirabilis.*

	Inhibition zone diameter			
Gram negative bacteria	Imipenem 20 µg	Amoxicillin/clavulanic 20/10 µg	Meropenem 10 µg	Piperacillin tazobactam 100/10 µg
K.Pneumoniae	26.00±1.00a	0.00 b	27.00±0.57a	26.33±0.33 a
E . coli	0.00 b	0.00 b	16.00±0.57a	0.00 b
P .mirabilis	B	17.00±0.57 b	26.67±0.67a	25.00±0.57 a
Sig (p. value)	0.001	0.001	0.001	0.001

The p-values ($p \leq 0.001$) indicate statistically significant differences between the treatments

Table 2. Inhibition zone diameter of AgNPs against *K. pneumoniae, E.coli,* and *P. mirabilis*

	AgNPs concentration			
Gram negative bacteria	1000 ppm	100 Ppm	10 ppm	1 ppm
	Inhibition zone diameter mm			
K.Pneumoniae	16.00±0.58 a	12.00±0.33 b	R	R
E . coli	22.33±0.33 a	20.00±0.57 ab	17.33±0.33 b	R
P .mirabilis	27.00±0.57a	17.67±0.33 b	16.00±0.57 b	R
Sig (p. value)	0.001	0.001	0.001	0.001

The p-values ($p \leq 0.001$) indicate statistically significant differences between the treatments. Same letter in the same column mean no significant differences between AgNPs concentration (mean±S.E)

4. Conclusion

This study successfully demonstrates a green synthesis route for silver nanoparticles (AgNPs) using *Candida albicans* supernatant as a natural reducing agent. Structural characterization confirmed the formation of face-centered cubic crystalline AgNPs. The biosynthesized nanoparticles exhibited potent, concentration-dependent antibacterial activity against *Klebsiella pneumoniae*, *Proteus mirabilis*, and *Escherichia coli*, with *P. mirabilis* showing the

highest susceptibility. Notably, AgNPs inhibited *E. coli* despite its resistance to conventional antibiotics such as piperacillin-tazobactam and amoxicillin-clavulanic acid. Differences in bacterial response may relate to variations in membrane composition and resistance mechanisms. Prior studies also suggest that AgNPs, especially when combined with antibiotics, are effective against resistant Gram-negative strains and biofilm-forming bacteria. The nanoscale size and spherical shape of the AgNPs, confirmed by FESEM and AFM, likely enhanced their bactericidal activity by increasing the surface area for microbial interaction [34]. These findings support the potential use of biosynthesized AgNPs in combating resistant bacterial infections. These findings underscore the potential of biologically synthesized AgNPs as effective alternatives in combating multidrug-resistant Gram-negative pathogens.

Credit Author Contributions Statement:

Nour Radhi Saud: Conceptualization, Methodology, Investigation, Data Curation, Formal Analysis, Visualization, Writing – Original Draft.

Mouna Akeel Hamed Al-Oebady: Supervision, Writing – Review & Editing, Validation, Project Administration.

Funding Statement:

The authors declare that no specific funding was received from any public, commercial, or not-for-profit funding agency for the conduct of this research.

Data availability statement:

The data supporting the findings of this study are available from the corresponding author upon reasonable request. The data are not publicly available due to privacy or ethical restrictions.

Conflict of Interest Statement:

The authors declare that there is no conflict of interest regarding the publication of this paper.

Ethical Approval (for studies in humans/animals)

Not applicable.

Informed Consent

Not applicable.

Acknowledgment. We thank the Microbiology Laboratory in Science College / Al Muthanna University for the use of their equipment**.**

References

[1] Diop, M.,et al., 2025, Prevalence of multidrug-resistant bacteria in healthcare and community settings in West Africa:

systematic review and meta-analysis," BMC Infect. Dis., 25, 292,.

[2] Elshobary, M. E., et al., 2025, Combating antibiotic resistance: Mechanisms, multidrug-resistant pathogens, and novel therapeutic approaches: An updated review, Pharmaceuticals, 18, 402,.

[3] Merker, M., et al., 2020, Evolutionary Approaches to Combat Antibiotic Resistance: Opportunities and Challenges for Precision Medicine, Aug.. doi: 10.3389/fimmu.2020.01938.

[4] Gajic, I., et al., 2025, A comprehensive overview of antibacterial agents for combating Multidrug-Resistant bacteria: the current landscape, development, future opportunities, and challenges, Antibiotics, 14, 221.

[5] Hetta, H. F., et al., 2023, Nanotechnology: a contemporary therapeutic approach in combating infections from multidrug-resistant bacteria, Biomedicines, 11, 413.

[6] Brar, B., Marwaha, S.,. Poonia, A. K, B., Koul, S. Kajla, and V. D. Rajput, 2023, Nanotechnology: a contemporary therapeutic approach in combating infections from multidrug-resistant bacteria, Arch. Microbiol., 205, 62. doi: 10.1007/s00203-023-03404-3.

[7] Bratovcic, A., 2020, Review on Metals and Metal Oxides in Sustainable Energy Production: Progress and PerspectivesClick to copy article link, Lead Chem., 10,.

[8] Farooq, U., Ahmad, T., Naaz, F., and S. ul Islam, 2023, Review on Metals and Metal Oxides in Sustainable Energy Production: Progress and Perspectives. doi: 10.1021/acs.energyfuels.2c03396.

[9] Mansor, M., Fatehah, M. O., H. A. Aziz, and L. K. Wang, 2024, Occurrence, behaviour and transport of heavy metals from industries in river catchments, in Industrial waste engineering, Springer, 205–277.

[10] Chauhan, S. B., and Singh, I., 2024, Nanotechnology-Based Approaches for Mitigating Antibacterial Resistance," in Contemporary Approaches to Mitigating Antibacterial Drug Resistance, IGI Global, 268–288.

[11] Karimadom, B. R.,and Kornweitz, H., 2021, Mechanism of producing metallic nanoparticles, with an emphasis on silver and gold nanoparticles, using bottom-up methods, Molecules, 26, 2968.

[12] Zahoor, M., et al., 2021, A review on silver nanoparticles: Classification, various methods of synthesis, and their

potential roles in biomedical applications and water treatment, Water, 13, 2216,.

[13] Ahmed, S. F.,et al., 2022, Green approaches in synthesising nanomaterials for environmental nanobioremediation: Technological advancements, applications, benefits and challenges, Environ. Res., 204, 111967,

[14] Ślusarczyk, J., Adamska, E., and Czerwik-Marcinkowska, J., 2021, Fungi and Algae as Sources of Medicinal and Other Biologically Active Compounds: A Review. doi: 10.3390/nu13093178.

[15] Eugenio, M., et al., 2016, Yeast-derived biosynthesis of silver/silver chloride nanoparticles and their antiproliferative activity against bacteria, Rsc Adv., 6, 9893–9904.

[16] Parasuraman, P., Busi, S., and J.-K. Lee, 2024, Standard microbiological techniques (Staining, Morphological and Cultural Characteristics, Biochemical Properties, and Serotyping) in the Detection of ESKAPE Pathogens, in ESKAPE Pathogens: Detection, Mechanisms and Treatment Strategies, Springer, 119–155.

[17] Hikmet, R. A.,and Hussein, N. N., 2021, Mycosynthesis of Silver Nanoparticles by Candida albicans Yeast and its Biological Applications., Arch. Razi Inst., 76, 857–869. doi: 10.22092/ari.2021.355935.1741.

[18] Hassanien, A. S. and Khatoon, U. T., 2019, Synthesis and characterization of stable silver nanoparticles, Ag-NPs: Discussion on the applications of Ag-NPs as antimicrobial agents, Phys. B Condens. Matter, 554, 21–30,

[19] Sadeghi, E., Taghavi, R., Hasanzadeh, A., and Rostamnia, S., 2024, Bactericidal behavior of silver nanoparticle decorated nano-sized magnetic hydroxyapatite, Nanoscale Adv., 6, 6166–6172,

[20] Raja, M. K., XRD line profile analysis for understanding the influence of cold work on ageing behaviour in 304HCu steel, 2020, Ph. D. Thesis, Homi Bhabha National Institute.

[21] Ghatage, M. M., et al., 2023, Green synthesis of silver nanoparticles via Aloe barbadensis miller leaves: Anticancer, antioxidative, antimicrobial and photocatalytic properties, Appl. Surf. Sci. Adv., 16, p 100426.

[22] Khan, S.,, Rukayadi, Y., Jaafar, A. H., and Ahmad, N. H., 2023, Antibacterial potential of silver nanoparticles (SP-AgNPs) synthesized from Syzygium polyanthum (Wight) Walp. against selected foodborne

pathogens,Heliyon, 9, doi: 10.1016/j.heliyon.2023.e22771.

[23] Salman, B. H., 2021, antibacterial and antibiofilm detection of some plant extracts against Escherichia coli ATCC 25922 and Escherichia coli ATCC 35218.

[24] Yao, H., Liu, J., Jiang, X., Chen, F., X. Lu, and J. Zhang, 2021, Analysis of the clinical effect of combined drug susceptibility to guide medication for carbapenem-resistant klebsiella pneumoniae patients based on the kirby–bauer disk diffusion method, Infect. Drug Resist., 79–87,

[25] Hadid, W. W., and Abed, F. N., Phenotypic and molecular identification of some species of Candida spp, J Hyg Eng Des, 44, 2023.

[26] popovici, R., 2024, the highlighting of m-type colonies for klebsiella., Analele Univ. din Oradea, Fasc. Ecotoxicologie, Zooteh. si Tehnol. în Ind. Aliment., 23,

[27] de Souza, H. D. F. et al., 2024, Is green metallic sheen in emb agar accurate to assist the Escherichia coli identification?, Rev. Pró-UniverSUS, 15, 1–9,

[28] Gazel, D., H. Demirbakan, and M. Erinmez, 2021, In vitro activity of hyperthermia on swarming motility and antimicrobial susceptibility profiles of Proteus mirabilis isolates, Int. J. Hyperth., 38, 1002–1012.

[29] Prema, P., et al., 2022, solutions of AgNPs ,it has been checking of color change as indicator of synthesis of nano particles, Environ. Res., 204, 111915,

[30] Sun, S., Zhang, X., J, Cui, and S. Liang, 2020, Identification of the Miller indices of a crystallographic plane: a tutorial and a comprehensive review on fundamental theory, universal methods based on different case studies and matters needing attention, Nanoscale, 12, 16657–16677,

[31] Saqib, S., et al., 2022, Bimetallic Assembled Silver Nanoparticles Impregnated in Aspergillus fumigatus Extract Damage the Bacterial Membrane Surface and Release Cellular Contents, doi: 10.3390/coatings12101505.

[32] Aldosari, B. N., et al., 2023, Synthesis and characterization of magnetic Ag–Fe3O4@ polymer hybrid nanocomposite systems with promising antibacterial application, Drug Dev. Ind. Pharm., 49, 723–733,

[33] Ahlburg, J. V., 2020. Realising Sample Environments for X-ray and Neutron Powder Diffraction: Demonstrated through In Situ Studies of Magnetic Ferrites.

[34] Ali, S., et al., 2020, Bioinspired morphology-controlled silver nanoparticles for antimicrobial application, Mater. Sci. Eng. C, 108, 110421.

[35] Palau, M., et al., 2023, In vitro antibacterial activity of silver nanoparticles conjugated with amikacin and combined with hyperthermia against drug-resistant and biofilm-producing strainsMicrobiol. Spectr., 11, e00280-23.

[36] Sheng, Y., et al., 2022, In vitro and in vivo efficacy of green synthesized AgNPs against Gram negative and Gram positive bacterial pathogens, Process Biochem., 112, 241–247,